

High-Pressure Densities of Ethane, Pentane, Pentane- d_{12} , 25.5 wt % Ethane in Pentane- d_{12} , 2.4 wt % Deuterated Poly(ethylene-*co*-butene) (PEB) in Ethane, 5.3 wt % Hydrogenated PEB in Pentane, 5.1 wt % Hydrogenated PEB in Pentane- d_{12} , and 4.9 wt % Hydrogenated PEB in Pentane- d_{12} + 23.1 wt % Ethane

H.-S. Byun,[†] T. P. DiNoia,[‡] and M. A. McHugh^{*,§}

Department of Chemical Engineering, Yosu National University, Yosu, Chonnam 550-749, South Korea,
 Department of Chemical Engineering, Johns Hopkins University, Baltimore, Maryland 21218, and
 Department of Chemical Engineering, Virginia Commonwealth University, Richmond, Virginia 23284

Densities at 30–150 °C and pressures to 3000 bar are reported for ethane, *n*-pentane, *n*-pentane- d_{12} , *n*-pentane- d_{12} + 25.5 wt % ethane, and mixtures of poly(ethylene-*co*-butene) (PEB) in ethane, and PEB in *n*-pentane, in *n*-pentane- d_{12} , and in an *n*-pentane- d_{12} + 23.1 wt % ethane mixture. The density data are measured with a high-pressure variable volume cell adapted with a linear-variable differential transducer. A detailed comparison is performed for the experimentally measured densities obtained in this work to experimental data available in the literature and to correlations reported in the literature for *n*-pentane. The experimental densities reported in this work have an estimated experimental uncertainty of 1.0–1.5%.

Introduction

Small-angle neutron scattering (SANS) has recently been used to characterize intra- and intermolecular interactions of slightly branched poly(ethylene-*co*-butene) (PEB) polymers in supercritical fluid (SCF) and liquid solvents at high pressures (*1*). Accurate densities of the SCF-polymer solutions are needed to properly extract polymer chain dimensions from scattering data and to account for compressibility effects on the scattering intensities. Unfortunately, there is a very limited amount of data available in the literature on the densities for these solutions under such extreme conditions. This paper provides experimentally determined densities for both protonated and deuterated *n*-alkanes and semidilute solutions of protonated and deuterated poly(ethylene-*co*-butene) in protonated and deuterated *n*-alkanes at pressures to 3000 bar and temperatures to 150 °C. Density differences will exist between mixtures consisting of deuterated and protonated components as compared to mixtures consisting of all hydrogenated components since pairwise intermolecular interactions will be slightly different in these two types of mixtures. For the density measurements reported here, a high-pressure variable volume cell is adapted with a linear-variable differential transducer (LVDT) to measure the cell volume at different temperatures and pressures.

Experimental Section

Figure 1 shows a schematic diagram of the high-pressure cell used in this study. The body of the cell is constructed of a high nickel content steel (Nitronic 50) that has a 5.7

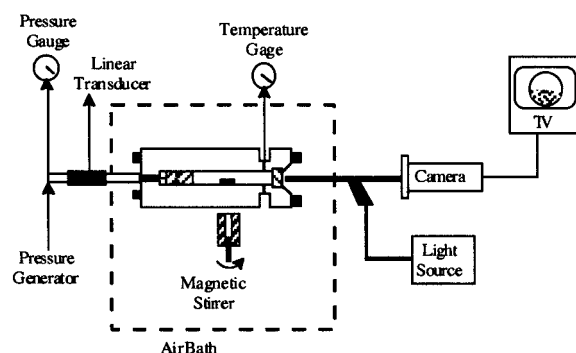


Figure 1. Schematic diagram of the experimental apparatus used in this study.

cm o.d. by 1.59 cm i.d. and a 35 cm³ working volume. A 1.9 cm o.d. by 1.9 cm thick sapphire window is fitted to one end of the cell and is sealed with an elastomeric O-ring. The cell contents are compressed to the desired operating pressure by displacing a piston in the cell using water pressurized with a high-pressure generator (HIP Inc., model 37-5.75-60). The system pressure is the water pressure measured with a Heise gauge (Dresser Industries, Heise model CM-108952, accurate to within ± 3.5 bar) plus the 1 bar of pressure needed to move the piston toward the back of the cell. The location of the piston is determined with an LVDT coil (Lucas Schaevitz Co., model 2000-HR) that fits around a 1.43 cm high-pressure tube and tracks the magnetic tip of a steel rod connected to the piston. The transducer coil is anchored to the 1.43 cm tube so that the initial reading is zero when the piston is close to the window of the cell, and it increases to $\sim 20\,000 \pm 5$ when the piston travels several inches toward the back of the cell. The temperature of the cell is measured with a type-E thermocouple (Omega Engineering, Inc.) that is accurate to within ± 0.5 °C and is connected to a digital multimeter

* To whom correspondence should be addressed. Phone: (804) 827-7031. Fax: (804) 828-4269. E-mail: mmchugh@saturn.vcu.edu.

[†] Yosu National University.

[‡] Johns Hopkins University.

[§] Virginia Commonwealth University.

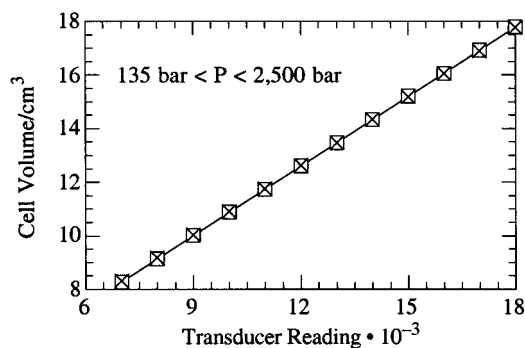


Figure 2. Calibration curve of the high-pressure, variable volume view cell with CO₂ at 40 °C for two independent calibration runs (open squares and crosses) performed 1 year apart.

(Omega, model DP462). A PID temperature controller (Fuji Electric, model PYZ4) connected to a platinum resistance temperature device (RTD) (Omega) controls the temperature of the surrounding air bath and cell within ± 0.3 °C. A stir bar activated by a magnet located below the cell mixes the contents of the cell, and the calibration is performed with the stir bar in the cell.

Pure CO₂ is used to calibrate the transducer since an accurate, and easy to use, density equation is available (2). After the stir bar is placed into the cell, the end caps are secured, and the cell is purged three times with nitrogen at ~ 25 bar and then three times with CO₂ at ~ 25 bar. Typically 12 ± 0.01 g of CO₂ (bone dry grade, 99.8% minimum purity, Potomac Airgas Inc.) is loaded into the cell at room conditions for the calibration measurements. The pressure in the cell is increased to ~ 125 bar at a temperature of 40 ± 0.3 °C, and the transducer reading is recorded. Transducer readings are obtained at pressure steps of ~ 75 bar up to 425 bar and are then obtained at pressure steps of ~ 150 bar up to 2500 bar. At a given temperature, pressure, and transducer reading, the volume of the cell is determined by dividing the mass of CO₂ loaded into the cell by the specific density of CO₂ calculated with the correlation of Michels and Michels (2). The calibration is repeated with a new loading of CO₂ at room temperature and at ~ 120 °C to determine the experimental reproducibility of the technique.

Figure 2 shows that a reproducible, linear calibration curve is obtained with this technique. The accumulated uncertainty of the volume measurement is determined by accounting for uncertainty in the mass loading of CO₂ (± 0.01 g), the uncertainty of the calculated density obtained from the correlation given by Michels and Michels (2) (~ 0.5 – 1.5%), the uncertainty in the measured pressure and temperature, the sensitivity of the LVDT, and the uncertainty from the least squares fit of the linear calibration curve. The densities presented here have an estimated accumulated uncertainty of 1.0–1.5% for pressures to 3000 bar and temperatures to 150 °C.

Materials

Ethane (99.0% minimum purity) was obtained from Aldrich Chemical Co., *n*-pentane (99.7% minimum purity) was obtained from Fisher Chemicals, and *n*-pentane-*d*₁₂ (98.0% minimum purity—D, 98%) was obtained from Cambridge Isotopes Laboratories. Pamela Wright and Lewis Fetters of Exxon Research and Engineering Co. provided protonated and partially deuterated poly(ethylene-*co*-butene) copolymers. The PEB copolymers were produced from anionic polymerization of polybutadiene along with subsequent saturation through hydrogenation or deuteria-

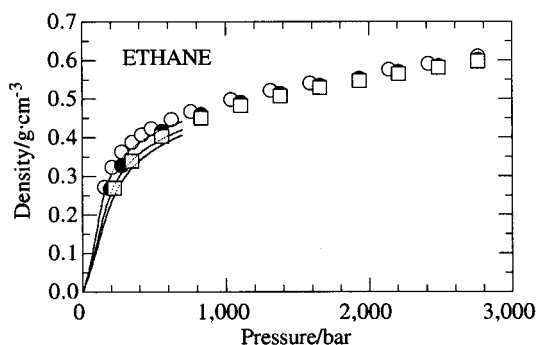


Figure 3. Comparison of experimental densities of ethane obtained in this study to those calculated from the SWEOS recommended by Friend et al. (7) at 100 (open circles), 130 (closed circles), and 150 °C (open squares).

Table 1. Experimental Densities of Ethane

pressure/bar	Density/(g·cm ⁻³)		
	<i>t</i> = 100 °C	<i>t</i> = 130 °C	<i>t</i> = 150 °C
154.8	0.273		
194.8		0.268	
208.6	0.323		
222.4			0.269
277.5	0.364	0.328	
346.5	0.389		0.340
415.4	0.408		
484.4	0.423		
553.3		0.416	0.402
622.2	0.448		
760.1	0.468		
829.1		0.460	0.449
1035.9	0.498		
1104.9		0.491	0.482
1311.7	0.522		
1380.7		0.515	0.508
1587.5	0.542		
1656.4		0.536	0.529
1932.2		0.554	0.548
2139.1	0.576		
2208.0		0.570	0.565
2414.9	0.591		
2483.8		0.586	0.581
2759.6	0.610	0.601	0.597

tion. Details of the polymerization and saturation processes are described elsewhere (3–6). Fully protonated and partially deuterated poly(ethylene-*co*-20.2 mol % butene) have weight-average molecular masses (M_w) of 232 500 and 245 000, respectively, and molecular mass distributions (M_w/M_n) of 1.01. The 20.2 mol % butene content corresponds to 10 ethyl branches per 100 backbone carbon atoms, and the protonated and partially deuterated PEB copolymers are labeled h-PEB-10 and d-PEB-10, respectively. Fully deuterated poly(ethylene-*co*-3 mol % butene) ($D = 99.8\%$) was obtained from Polymer Sources, Inc., with an $M_w = 169 000$ and an M_w/M_n of 1.09. This copolymer was produced from catalytic polymerization of deuterated 1,3-butadiene monomer. The degree of ethyl side chain branching was controlled by the amount of 1,2-addition in the polymerization process. The polybutadiene was fully deuterated in the presence of a D₂ at 26 bar and 60 °C for 24 h. The 3 mol % butene content corresponds to approximately two ethyl branches per 100 backbone carbon atoms. This polymer is labeled d-PEB-2.

Results and Discussion

Table 1 lists the experimental densities for ethane at 100, 130, and 150 °C for pressures up to 2760 bar. Figure 3 shows a comparison of ethane densities obtained here to

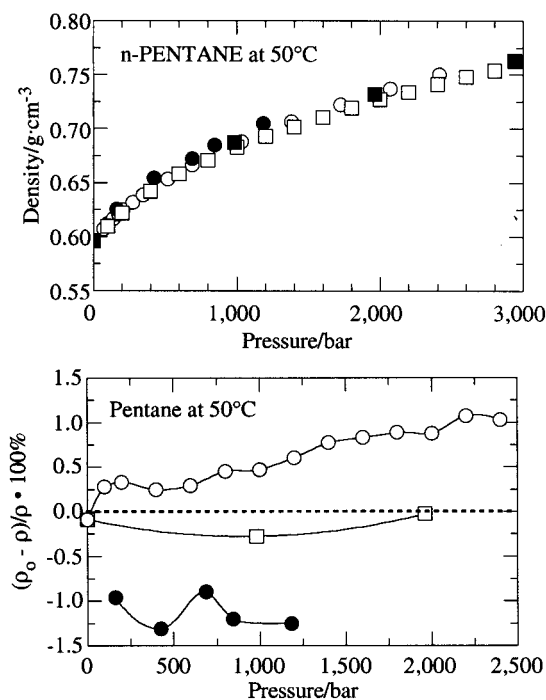


Figure 4. (a, top) Density behavior of *n*-pentane obtained in this work (open circles) compared to the data of Bridgman (8) (closed squares), Gehrig and Lentz (9) (closed circles), and Eastale and Woolf (10) (open squares) at 50 °C and pressures to 3000 bar. (b, bottom) Percentage difference between the density of pentane obtained in this study, ρ_0 , as determined from an eight-order fit of the data, to the densities obtained by Bridgman (8) (open squares), Gehrig and Lentz (9) (closed circles), and Eastale and Woolf (10) (open circles).

Table 2. Experimental Densities of *n*-Pentane

pressure/ bar	Density/(g·cm ⁻³)					
	<i>t</i> = 50 °C	<i>t</i> = 75 °C	<i>t</i> = 100 °C	<i>t</i> = 110 °C	<i>t</i> = 130 °C	<i>t</i> = 150 °C
70.7	0.607	0.583	0.558	0.550	0.526	0.503
105.1	0.613	0.591	0.568	0.559	0.538	0.516
139.6	0.617	0.597	0.575	0.567	0.546	0.526
174.1	0.621	0.602	0.581	0.573	0.554	0.536
208.6	0.625	0.606	0.586	0.579	0.561	0.544
277.5	0.632	0.615	0.596	0.589	0.573	0.558
346.5	0.639	0.622	0.604	0.598	0.583	0.569
518.8	0.654	0.638	0.622	0.617	0.604	0.592
689.5	0.666	0.653	0.637	0.632	0.621	0.610
1034.2	0.688	0.676	0.663	0.658	0.648	0.639
1380.7	0.707	0.695	0.683	0.679	0.671	0.662
1725.4	0.723	0.712	0.701	0.698	0.690	0.682
2070.1	0.737	0.727	0.717	0.714	0.707	0.699
2414.9	0.750	0.741	0.732	0.728	0.722	0.715

those calculated with the Schmidt–Wagner equation of state (7) (SWEOS) for pressures up to 700 bar. The largest difference between experimental and calculated densities is 3.0, 4.0, and 5.0% at 700 bar and 100, 130, and 150 °C, respectively. The densities obtained from the SWEOS have an estimated accuracy of 0.2–0.5%; however, only a limited amount of data at temperatures greater than 100 °C and pressure to 550 bar were involved in the evaluation of the equation of state.

Table 2 lists the experimental densities of *n*-pentane at 50, 75, 100, 110, 130, and 150 °C for pressures up to 2415 bar. Figure 4a shows a comparison of *n*-pentane densities at 50 °C obtained in this study with the data of Bridgman (8), Gehrig and Lentz (9), and Eastale and Woolf (10). All the data sets are within 0.8% of each other over the entire pressure range. The densities reported are slightly lower

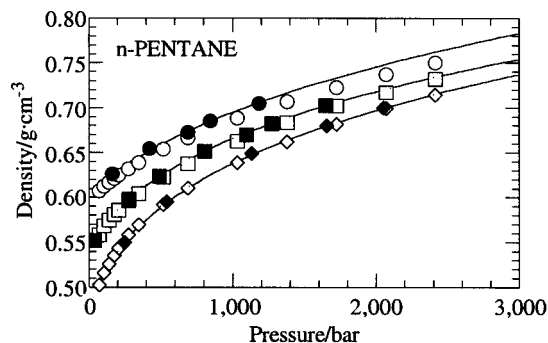


Figure 5. Density behavior of *n*-pentane obtained in this work (open symbols) compared to the experimental data of Gehrig and Lentz (9) (closed symbols) and to calculated values from the Tait equation provided by Gehrig and Lentz (9) (smooth curves) at 50 (circles), 100 (squares), and 150 °C (diamonds).

than those of Gehrig and Lentz, they are slightly higher than those of Eastale and Woolf for pressures greater than ~700 bar, and they agree very well with the data of Bridgman. Figure 4b shows that the densities measured in this study are within $\pm 1.5\%$ of those reported in the literature.

The Tait equation provided by Gehrig and Lentz (9) is the only correlation in the literature that is in close agreement with the data in this study for *n*-pentane at temperatures above 50 °C and pressures greater than 700 bar. Figure 5 shows the densities of *n*-pentane obtained in this work compared to experimental data and the calculated values from the Tait equation of Gehrig and Lentz at 50, 100, and 150 °C. Except for the 50 °C data, the correlation for *n*-pentane agrees to within 0.1–0.5% of the data reported here for pressures up to 2500 bar. Eastale and Woolf note that there appears to be a systematic uncertainty in the data of Gehrig and Lentz at 50 °C, and this suggestion supports the observation of Kratzke and co-workers (11), who state that all of the data of Gehrig and Lentz are only accurate to within 0.3–1.7%. The high-pressure densities at 50 °C reported here agree within this 1.7% accuracy margin.

The Tait equation for *n*-pentane provided by Assael and co-workers (12) only agrees with the *n*-pentane densities reported here at 50 °C and at pressures less than 500 bar. At higher pressures the experimental pentane densities differ from those calculated from the Tait equation by considerably more than 0.10%, the reported average accuracy of this equation. However, Assael and co-workers report parameters for the Tait equation that are determined from a generalized fit to a series of *n*-alkanes ranging from methane to *n*-hexadecane and to a limited amount of high-pressure densities for *n*-pentane. In addition, the parameters for *n*-pentane at atmospheric pressure reported by Assael and co-workers are also incorrect or misprinted from the original publication of Cibulka (13).

The *n*-pentane data agree with the correlation of Cibulka and Hnedkovsky (14) for temperatures up to 150 °C and pressures less than 700 bar with a maximum deviation of approximately 0.8%. At higher pressures, the correlation underpredicts the densities for all isotherms and the deviation increases with increasing temperature. Maximum deviations of 1.5, 2.0, and 2.2% are found between the experimental data reported here and calculated densities at pressures from 700 to 2500 bar and temperatures of 50, 100, and 150 °C, respectively. These deviations at high pressures are not unexpected since the Tait equation reported by Cibulka and Hnedkovsky, fit to the only four available data sets that report *n*-pentane densities at

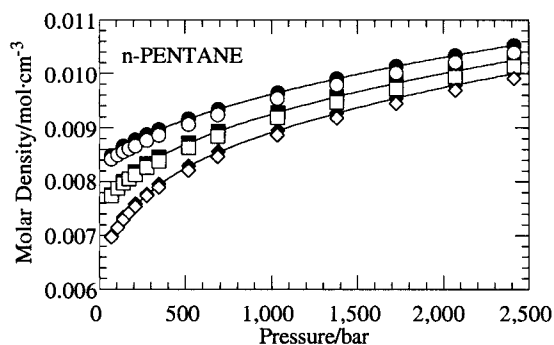


Figure 6. Molar densities of *n*-pentane-*d*₁₂ (closed symbols) compared to *n*-pentane-*h*₁₂ (open symbols) obtained in this study at temperatures of 50 (circles), 100 (squares), and 150 °C (diamonds).

Table 3. Experimental Densities of *n*-Pentane-*d*₁₂

pressure/ bar	Density/(g·cm ⁻³)						
	<i>t</i> = 30 °C	<i>t</i> = 50 °C	<i>t</i> = 75 °C	<i>t</i> = 100 °C	<i>t</i> = 110 °C	<i>t</i> = 130 °C	<i>t</i> = 150 °C
56.9	0.737						
70.7	0.739	0.714	0.686	0.653	0.644	0.615	0.588
105.1	0.743		0.696			0.629	
139.1	0.748	0.728	0.703	0.673	0.664	0.640	0.617
174.1	0.752		0.709			0.649	
208.6	0.756	0.738	0.714	0.689	0.679	0.658	0.638
243.0	0.760						
277.5	0.764	0.746	0.724	0.701	0.692	0.672	0.654
346.5	0.771	0.754	0.733	0.712	0.703	0.685	0.669
518.8	0.787	0.771	0.753	0.734	0.727		0.698
691.2	0.801	0.786	0.769	0.752	0.746	0.732	0.719
1035.9	0.825	0.812	0.797	0.781	0.776	0.763	0.753
1380.7	0.846	0.834	0.820	0.806	0.801	0.789	0.780
1725.4	0.864	0.853	0.840	0.827	0.822	0.812	0.803
2070.1	0.881	0.871	0.858	0.846	0.841	0.833	0.824
2414.9	0.896	0.886	0.874	0.863	0.859	0.851	0.842

Table 4. Experimental Densities of *n*-Pentane-*d*₁₂ + 25.5 wt % Ethane

pressure/bar	Density/(g·cm ⁻³)		
	<i>t</i> = 110 °C	<i>t</i> = 130 °C	<i>t</i> = 150 °C
105.1	0.564		
132.7		0.549	
139.6	0.580	0.552	
174.1	0.593	0.567	
198.2			0.550
208.6	0.604	0.579	0.556
243.0			0.569
277.5	0.623	0.600	0.580
346.5	0.639	0.618	0.598
518.8	0.670	0.653	0.636
691.2	0.693	0.678	0.664
1035.9	0.729	0.716	0.705
1380.7	0.757	0.746	0.735
1725.4	0.781	0.771	0.761
2070.1	0.801	0.792	0.782
2414.9	0.819	0.810	0.802

temperatures from 50 to 150 °C and pressures from 700 to 2500 bar, has a root mean square deviation of 0.12–2.09%.

Table 3 lists the densities of *n*-pentane-*d*₁₂ at 30, 50, 75, 100, 110, 130, and 150 °C and pressures to 2415 bar. The specific density of *n*-pentane-*d*₁₂ is greater than that of *n*-pentane-*h*₁₂ at the same pressures and temperatures. Figure 6 shows that the molar density of *n*-pentane-*d*₁₂ is consistently slightly greater than the molar density of *n*-pentane-*h*₁₂. This trend in molar density is consistent with studies in the literature (15–17), reporting that deuteration of a hydrocarbon slightly reduces the polarizability of the compound but increases the molar density

Table 5. Experimental Densities of Ethane + 2.4 wt % *d*-PEB-2

pressure/bar	Density/(g·cm ⁻³)		
	<i>t</i> = 120 °C	<i>t</i> = 130 °C	<i>t</i> = 150 °C
1173.8			0.489
1242.8	0.511	0.506	0.497
1311.7	0.518	0.513	0.503
1380.7	0.523	0.518	0.508
1518.5	0.532	0.528	0.519
1725.4	0.546	0.541	0.533
1897.8	0.554	0.551	0.543
2070.1	0.563	0.561	0.553
2242.5	0.571	0.570	0.562
2414.9	0.580	0.578	0.571

Table 6. Experimental Densities of *n*-Pentane + 5.3 wt % *h*-PEB-10

pressure/bar	Density/(g·cm ⁻³)		
	<i>t</i> = 110 °C	<i>t</i> = 130 °C	<i>t</i> = 150 °C
45.2		0.528	
70.7	0.560	0.536	
105.1			0.525
139.6	0.575	0.555	0.535
208.6	0.586	0.569	0.552
277.5	0.596	0.581	0.566
346.5	0.605	0.591	0.577
415.4		0.599	
484.4		0.607	
518.8	0.623		0.599
553.3		0.614	
622.2		0.621	
691.2	0.638	0.627	0.617
760.1		0.633	
829.1		0.639	
898.0		0.644	
967.0		0.649	
1035.9	0.664	0.654	0.645
1104.9		0.659	
1173.8		0.663	
1242.8		0.668	
1311.7		0.672	
1380.7	0.685	0.676	0.668
1449.6		0.680	
1518.5		0.684	
1587.5		0.688	
1656.4		0.691	
1725.4		0.695	
1794.3		0.698	
1863.3		0.702	
1932.2		0.705	
2001.2		0.708	
2070.1	0.719	0.712	0.704
2414.9	0.733		0.720

due to a smaller C–D bond length relative to a C–H bond. The maximum difference in molar densities of *n*-pentane-*d*₁₂ compared to *n*-pentane-*h*₁₂ is ~0.7% for 50, 100, and 150 °C for all pressures up to 2415 bar.

Table 4 lists the experimental densities for a mixture of *n*-pentane-*d*₁₂ + 25.5 wt % ethane at 110, 130, and 150 °C and pressures to 2500 bar. Not surprisingly, the mixture density is less than the density of pure *n*-pentane-*d*₁₂ at the same temperature and pressure. Table 5 lists the density of ethane + 2.4 wt % *d*-PEB-2 at temperatures of 120, 130, and 150 °C and pressures from 1174 to 2415 bar. These densities differ only slightly from those of pure ethane at the same conditions. Tables 6 and 7 list the densities of *n*-pentane + 5.3 wt % *h*-PEB-10 and of *n*-pentane-*d*₁₂ + 5.1 wt % *h*-PEB-10, respectively, for isotherms at 110, 130, and 150 °C and pressures to 2415 bar. The densities of the *n*-pentane-*d*₁₂ + 5.1 wt % *h*-PEB-10 system are greater than those of the *n*-pentane-*h*₁₂ + 5.3 wt % *h*-PEB-10 at the same temperatures and pres-

Table 7. Experimental Densities of *n*-Pentane-*d*₁₂ + 5.1 wt % h-PEB-10

pressure/bar	Density/(g·cm ⁻³)		
	<i>t</i> = 110 °C	<i>t</i> = 130 °C	<i>t</i> = 150 °C
70.7	0.644	0.617	
77.6		0.619	
84.5		0.621	
91.3		0.624	
105.1		0.628	
108.6			0.605
125.8		0.634	
139.6	0.662	0.638	0.616
174.1		0.647	
208.6	0.676	0.655	0.635
277.5	0.688	0.669	0.651
346.5	0.699	0.681	0.664
518.8	0.722	0.705	0.692
689.5		0.725	
691.2	0.740		0.714
1034.2		0.757	
1035.9	0.771		0.747
1380.7	0.796	0.783	0.774
2070.1	0.837	0.826	0.818
2414.9	0.855	0.844	0.837

Table 8. Experimental Densities of *n*-Pentane-*d*₁₂ + 23.1 wt % Ethane + 4.9 wt % h-PEB-10

pressure/bar	Density/(g·cm ⁻³)		
	<i>t</i> = 110 °C	<i>t</i> = 130 °C	<i>t</i> = 150 °C
277.5	0.643	0.622	
312.0	0.650	0.630	
346.5	0.656	0.634	0.619
380.9	0.662	0.645	0.627
415.4	0.667	0.651	0.634
484.3	0.677	0.662	0.646
553.3	0.687	0.672	0.657
691.2	0.702	0.689	0.676
1035.9	0.736	0.724	0.712
1380.7	0.762	0.752	0.741
1725.4	0.785	0.775	0.765
2070.1	0.805	0.796	0.786
2414.9	0.822	0.814	0.805

tures. Table 8 lists the densities for the *n*-pentane-*d*₁₂ + 23.1 wt % ethane + 4.9 wt % h-PEB-10 system.

Conclusions

Densities are reported for pure ethane, *n*-pentane, *n*-pentane-*d*₁₂, and *n*-pentane-*d*₁₂ + ethane mixtures with protonated and deuterated polyolefins for pressures up to 3000 bar and temperatures to 150 °C. Good agreement is found for *n*-pentane densities obtained here at 50 °C and pressures to 3000 bar with the data of Bridgman (8), Gehrig and Lentz (9), and Easteal and Woolf (10). The densities obtained in this study have an estimated accumulated uncertainty of 1.0–1.5%, which may be a conservative estimate based on comparisons with *n*-pentane data obtained from the literature. The density data reported here provide information at higher pressures and temperatures than those currently found in the literature.

Acknowledgment

The authors thank Pamela Wright and Lewis Fetters for providing the h-PEB-10 and d-PEB-10 polymer samples used in this work. T.P.D. and M.A.M. acknowledge the National Science Foundation for partial support under Grants CTS-99729720 and GER-9454136. H.-S.B. thanks the Korea Science and Engineering Foundation for financial support for this project.

Literature Cited

- (1) DiNoia, T. P.; Kirby, C. F.; van Zanten, J. H.; McHugh, M. A. Small-Angle Neutron Scattering of Polymer-Supercritical Fluid Solutions: Transitions from Liquid to Supercritical Fluid Solvent Quality. *Macromolecules*, submitted for publication.
- (2) Michels, A.; Michels, C. Series Evaluation of the Isotherm Data of CO₂ between 0 and 150 °C and up to 3000 atm. *Proc. R. Soc. London S., A* **1937**, *160*, 348–357.
- (3) Fetters, L. J.; Graessley, W. W.; Krishnamoorti, R.; Lohse, D. J. Melt Chain Dimensions of Poly(ethylene-1-butene) Copolymers via Small-Angle Neutron Scattering. *Macromolecules* **1997**, *30*, 4973–4977.
- (4) Balsara, N. P.; Fetters, L. J.; Hadjichristidis, N.; Lohse, D. J.; Han, C. C.; Graessley, W. W.; Krishnamoorti, R. Thermodynamic Interactions in Model Polyolefin Blends Obtained by Small-Angle Neutron Scattering. *Macromolecules* **1992**, *25*, 6137–6147.
- (5) Krigas, T. M.; Carella, J. M.; Struglinski, M. J.; Crist, B.; Graessley, W. W. Model Copolymers of Ethylene with Butene-1 Made by Hydrogenation of Polybutadiene: Chemical Composition and Selected Physical Properties. *J. Polym. Sci., Polym. Phys. Ed.* **1985**, *23*, 509–520.
- (6) Rachapudy, H.; Smith, G. G.; Raju, V. R.; Graessley, W. W. Properties of Amorphous and Crystallizable Hydrocarbon Polymers. III. Studies of the Hydrogenation of Polybutadiene. *J. Polym. Sci., Polym. Phys. Ed.* **1979**, *17*, 1211–1222.
- (7) Friend, D. G.; Ingham, H.; Ely, J. F. Thermophysical Properties of Ethane. *J. Phys. Chem. Ref. Data* **1991**, *20*, 275–348.
- (8) Bridgman, P. W. The Volume of Eighteen Liquids as a Function of Pressure and Temperature. *Proc. Am. Acad. Arts Sci.* **1931**, *66*, 185–233.
- (9) Gehrig, M.; Lentz, H. Values of p(V,T) for *n*-Pentane in the Range of 5 to 250 MPa and 313 to 643 K. *J. Chem. Thermodyn.* **1979**, *11*, 291–300.
- (10) Easteal, A. J.; Woolf, L. A. Volume Ratios for *n*-Pentane in the Temperature Range 278–338 K and at Pressures up to 280 MPa. *Int. J. Thermophys.* **1987**, *8*, 231–238.
- (11) Kratzke, H.; Muller, S.; Bohn, M.; Kohlen, R. Thermodynamic Properties of Saturated and Compressed Liquid *n*-Pentane. *J. Chem. Thermodyn.* **1985**, *17*, 283–294.
- (12) Assael, M. J.; Dymond, J. H.; Exadaktilou, D. An Improved Representation for *n*-Alkane Liquid Densities. *Int. J. Thermophys.* **1994**, *15*, 155–164.
- (13) Cibulka, I. Saturated Liquid Densities of 1-Alkanols from C1 to C10 and *n*-Alkanes from C5 to C16: A Critical Evaluation of Experimental Data. *Fluid Phase Equilib.* **1993**, *89*, 1–18.
- (14) Cibulka, I.; Hnedkovsky, L. Liquid Densities at Elevated Pressures of *n*-Alkane from C5 to C16: A Critical Evaluation of Experimental Data. *J. Chem. Eng. Data* **1996**, *41*, 657–668.
- (15) Rabinovich, I. B. Isotope Effect in Vapour Pressure. *Russ. Chem. Rev.* **1962**, *31*, 51–80.
- (16) Fenby, D. V.; Kooner, Z. S.; Khurma, J. R. Deuterium Isotope Effects in Liquid-Liquid Phase Diagrams: A Review. *Fluid Phase Equilib.* **1981**, *7*, 327–338.
- (17) Wade, D. Deuterium Isotope Effects on Noncovalent Interactions between Molecules. *Chemico-Biol. Int.* **1999**, *117*, 191–217.

Received for review December 8, 1999. Accepted May 19, 2000.

JE990308+